Underwater Depth Estimation and Image Restoration Based on Single Images

Paulo Drews-Jr, Erickson R. Nascimento, Silvia Botelho and Mario Campos

Images acquired in underwater environments undergo a degradation process due to the inherent complexity of the interaction of light with the medium. Such interaction includes numerous phenomena such as multipath refraction and reflection of light rays on particles in suspension with dynamic motion patterns. The complexity of a possibly complete model may render it unfeasible to be used in several applications which may requires frame rate performance. Thus, we have adopted a simplified model that takes into account the most significant effects to image degradation, *i.e.* absorption, scattering and backscattering. In this work, we present a restoration method based on a physical model of light propagation along the use of statistical priors of the scene. Our approach is able to simultaneously recover the medium transmission and the scene depth as well as to restore the visual quality of the images acquired in typical underwater scenarios.

Introduction

An increasing number of real-world applications are related to underwater environments, among which are fisheries, environmental and structural monitoring and inspections, and oil and gas exploration. Petroleum and natural gas are still the most important sources of energy in the world and researchers have recently discovered relevant oil and gas reserves along the coast of Brazil and Africa underneath what is known as pre-salt rock formations. Pre-salt layers of rocks in the earth's crust are composed only of petrified salt covering large areas on the ocean floor. Recent findings have unveiled that over millions of years large amounts of organic matter have been deposited beneath the layers of pressed salt between the west coast of Africa and the eastern shores of South America. This organic matter has been transformed into oil, which in many areas is engulfed with gas.

In Brazil, the pre-salt area spans a range of about 800 kilometers along the Brazilian coast. Geological studies have estimated that the oil and gas reserves in that area are in the order of 80 billion barrels, which would place Brazil as the sixth largest holder of reserves in the world – behind Saudi Arabia, Iran, Iraq, Kuwait and the United Arab Emirates.

Exploring and working in the pre-salt reserves present an important technological issue that includes the ability to perceive the underwater environment. Techniques based on machine vision can help humans to monitor and to supervise activities in these scenarios, as well as to enable carrying out missions with autonomous robotic vehicles. In general, computer vision algorithms assume that the medium does not affect light propagation. However, this assumption does not hold in scattering media such as underwater

scenes. Indeed, the phenomena of scattering and absorption affect the propagation of light, degrading the quality of the captured images.

Thus, the effort in the fields of image processing and computer vision for leading to an improvement in the quality of underwater images may contribute to several applications, especially those related to offshore oil and gas industry. In this paper, we address the problems of *image restoration*, to improve the visual quality of underwater images, and *depth estimation* of the scene to extract geometrical information of the objects in therein.

Image restoration and depth estimation are ambiguous problems, since in general the available number of constraints is smaller than the number of unknown variables. One of the strategies most commonly adopted to tackle these problems in computer vision is to impose extra constraints that are based on some *a priori* knowledge about the scene. These extra constraints are called *priors*. In general, a prior can be a statistical/physical property, *ad-hoc* rules, or even heuristic assumptions. The performance of the algorithms is limited by the extent to which the prior is valid. Some of the widely used priors in image processing are smoothness, sparsity, and symmetry.

Inspired by the observation of Kaiming He and colleagues [1] that natural scenes tend to be dark in at least one of the RGB color channels, we derived a new prior by making observations in underwater images on the relevance of the absorption rate in the red color channel. By collecting a large number of images from several image search engines, we tested our prior and show its applicability and limitations on images acquired from real scenes.

The main contribution of the work described in this paper is an extension of our previous work to deal with underwater image restoration called Underwater Dark Channel Prior (UDCP) [2]. We present a deeper study on the method, including an extensive statistical experimental verification of the assumption following the guidelines described in He and colleagues [1]. Additionally, we present a new application of the UDCP prior for underwater image restoration and depth estimation. We evaluated the algorithm using qualitative and quantitative analysis through a new set of data, including images acquired in the Brazilian coast. The techniques presented in this work open new opportunities to develop automatic algorithms for underwater applications that require high quality in visual information.

Previous Approaches in Image Restoration of Underwater Images

The works in literature have approached the problem of restoring images acquired from underwater scenes from several perspectives: using specific purpose hardware, stereo images and polarization filters [3]. Despite the improvements achieved by these approaches, they still present several limitations. For instance, methods that rely on specialized hardware are expensive and complex to be realized. The use of polarizers, for example, requires moving parts and it is hard to implement in automatic acquisition tasks. In a stereo vision system approach, the correspondence problem becomes even harder due to the strong

effects imposed by the medium. Methods based on multiple images require at least two images of the same scene taken under different environment conditions, which makes inadequate for real-time applications. Thus, the problem of image restoration for underwater scenes still demands much research effort in spite of the advances that have already been attained.

In the past few years, a large number of algorithms for image restoration based on single image have been proposed, and the works of He and colleagues [1] and of Raanan Fattal [4] the most cited in the field. While these works have shown good performance for enhancement in the visual quality for outdoor terrestrial images, there is still room for improvement when they are applied to underwater images. As far as single image methods are concerned, He and colleagues have proposed one of the most popular methods called Dark Channel Prior (DCP). Liu Chao and Meng Wang [5], John Chiang and Ying-Ching Chen [6], and Seiichi Serikawaa and Huimin Lu [7] have also applied the DCP method to restore the visual quality of underwater images. However, these works do not address some of the fundamental DCP limitations related with the absorption rate of the red channel, and do not discuss relevant issues with the basic DCP assumptions.

Differently than outdoor scenes, the underwater medium imposes wavelength dependent rates of absorption, mainly in the red channel. Thus, Paulo Drews-Jr and colleagues [2] proposed a modified version of the DCP to overcome this limitation of DCP prior for applications in underwater imaging. Here we build upon and extend the work presented in [2], providing an extensive study about the prior with applications to image restoration and depth estimation. Furthermore, we provide new results of image restoration using qualitative and quantitative analysis.

Underwater Attenuation Light Modelling

The underwater image formation results from a complex interaction between the light, the medium, and the scene. A simplified analysis of this interaction is possible, yet maintaining physical plausibility. To this end, first order effects are the *forward* scattering and the *back*scattering, *i.e.* the scattering of light rays in small and large angles. The absorption of light is associated with these two effects since they respond for contrast degradation and color shift in images. Fig. 1 illustrates these effects.

According to Yoav Schechner and Nir Karpel [3], backscattering is the prime reason for image contrast degradation, thus the forward scattering can be neglected. Therefore, the underwater attenuation light model is a linear combination of the direct light and the backscattering. The direct light is defined as the fraction of light irradiated by the scene where a part is lost due to scattering and absorption. On the other hand, the backscattering does not originate from the object's radiance, but it results from the interaction between the environment's illumination sources and the particles dispersed in the medium. For a homogeneous illuminated environment, the backscattered light can be assumed to be constant and it can be obtained from the image by using a completely haze-opaque region or by finding the farthest pixel in

the scene. However, this information is impossible to be automatically acquired from a single image. Finding the brightest pixel in the dark channel is assumed as an adequate approximation.

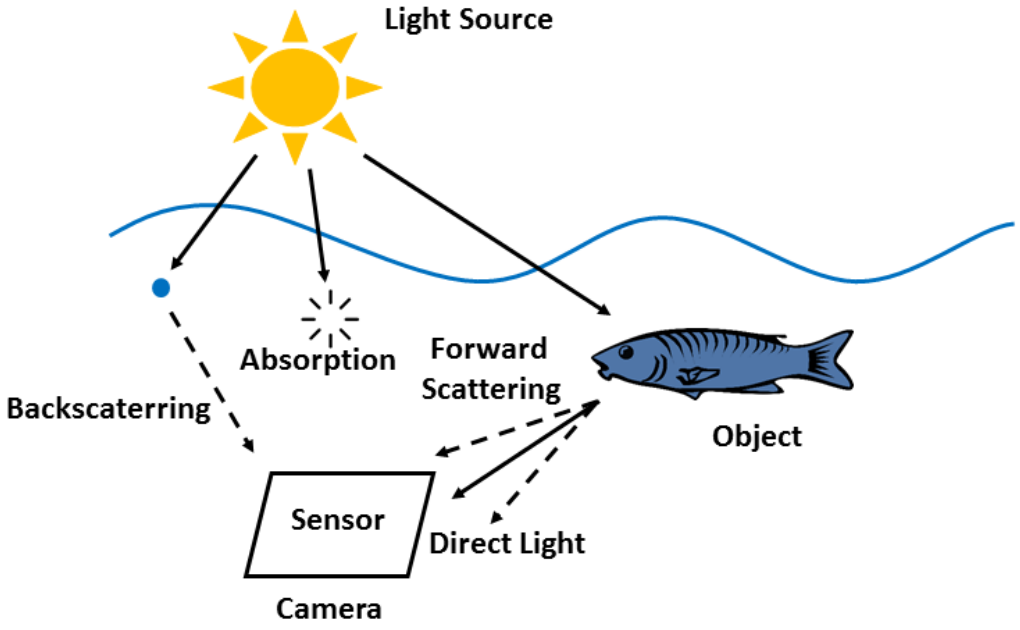

Fig. 1 – Diagram illustrating the underwater attenuation light model. The dashed lines show the forward scattering and backscattering effects. The scattering of light rays in small and large angles creates these effects, respectively. Direct light is the portion of light irradiated by the scene that reaches the image plane.

One important aspect of the linear model is the weight of the direct and of the backscattering components in the final image. The experimental analysis indicates an exponential behavior between the depth and the attenuation coefficient. This coefficient is an inherent property of the medium and it is defined as the sum of the absorption and scattering rates. Since both rates are wavelength dependent, the attenuation coefficient is different for each wavelength. In the literature exponential weight is called medium transmission. The depths in the scene are estimated up to a scale factor by applying the log operation to the medium transmission value.

The image restoration is performed by inverting the underwater attenuation light model. Assuming that we are able to estimate the medium transmission and the backscattering light, the restored image is computed by summing the backscattering light intensity and dividing it by the normalized color image.

Dark Channel Prior

The Dark Channel Prior is a statistical prior based on the observation that natural outdoor images in clear day exhibits mostly dark intensities in a square patch of the image [1]. This was inspired in the well-known dark-object subtraction method from the remote sensing field. The authors considered that in most of the non-sky patches on images of outdoor scenes, at least one color channel in the RGB representation would have some pixels whose intensity were almost zero. This low intensity in the dark channel was due to three factors: a) shadows in the images; b) colorful objects or surfaces where at least one color has low intensity and c) dark objects or surfaces. They collected a large number of outdoor images and built histograms, and with those, they have shown that about 75 percent of the pixels in the dark channel had zero values, and the intensity of 90 percent of the pixels was below 25 in a scale of [0;255]. Those results provide a strong support to the dark channel prior assumption for outdoor images. This prior allows the estimation of an approximation of the amount of the medium transmission in local patches. He and colleagues have shown that the Dark Channel provided excellent results in haze scenes.

The use of a local patch affects the performance of the medium transmission estimation. He and colleagues proposed the use of a spectral matting method to refine the estimated transmission. Their method presents good results but it requires a high computational effort to process the Laplacian matrix. Other works proposed approximate solutions to make it faster by using quadtrees, Markov Random Fields, or filtering techniques, e.g. guided filter or bilateral filter.

Dark Channel Prior on Underwater Images and its variations

Due to the good results obtained by the DCP method for haze scenes and the similarities in the modelling of a haze image and an underwater image, some previous works applied the Dark Channel Prior to process underwater images. One of the first works to use DCP in underwater images was Chao and Wang [5]. The reported results show a limited number of experiments where the visual quality of the results do not present a significant improvement, even for images with small degradation. Chiang and Chen [6] also proposed an underwater image restoration method using standard DCP. Their method obtained good results for real underwater images, but it was limited by the standard DCP method in underwater images and by the assumption that the image is predominantly blue. Recently, Serikawaa and Lu [7] proposed a variation of the DCP that filters the medium transmission by using Joint Trilateral Filter. Despite the improvement attained in the image restoration when compared to standard DCP, the limitation related to the red channel remains the same.

Kristofor Gibson and colleagues [8] proposed a variation of the DCP where they replaced the minimum operator in an image patch by the median operator. They named the method as MDCP. They chose the median operator due to its ability to preserve edges. Their approach could provide good estimation when the effects of the medium are approximately wavelength independent; in this case, the behavior tends to be similar to standard DCP.

Nicholas Carlevaris-Bianco and colleagues [9] proposed an underwater image restoration using a new interpretation of the DCP for underwater conditions. The proposed prior explores the fact that the attenuation of light in water varies depending on the color of the light. Underwater medium attenuates the red color channel at a much higher rate than the green and blue channels. Differently from the standard DCP, that prior is based on the difference between the maximum in the red channel and each one of the other channels (G and B), instead of with only the minimum as in DCP. The method works well when the absorption coefficient of the red channel is large. The method shows some shortcomings to estimate the medium transmission in typical shallow waters.

Underwater Dark Channel Prior and the Image Restoration

The statistical correlation of a low Dark Channel in haze-free images is not easy to be tested for underwater images due to the difficulty to obtain real images of underwater scene in an out-of-water condition. However, the assumptions made by He and colleagues are still plausible*, i.e.* at least one color channel has some pixels whose intensity are close to zero. These low intensities are due to a) shadows; b) color objects or surfaces having at least one color channel with low intensity, *e.g.* fishes, algae or corals; c) dark objects or surfaces, e.g. rocks or dark sediment.

Despite the fact that dark channel assumption seems to be correct, some problems arise from the wavelength independence assumption. There are many practical situations where the red channel is nearly dark, which corrupts the transmission estimate by the standard DCP. Indeed, the red channel suffers an aggressive decay caused by the absorption of the medium making it to be approximately zero even in shallow waters. Thus, the information of the red channel is undependable.

We proposed a new prior that considers just the green and the blue color channels to overcome this issue. We named this prior Underwater Dark Channel Prior (UDCP). This prior allows us to invert the model and to obtain an estimate of the medium transmission. The medium transmission and the backscattering light constants provide enough information to restore the images.

We performed an experimental verification to evaluate the assumption of the new prior based on two assumptions: a) the main assumption of the DCP for outdoor scenes remains valid if only applied to green and blue channels, and b) the behavior of the UDCP histogram in underwater scenes is plausible.

Since He's dataset has not be made publicly available, we created our own following the guidelines proposed by He and colleagues in [1]. The dataset is composed of 1,022 outdoor landscape images greater than 0.2 Mpixels from the SUN database [10], see Fig. 2 for image samples. We selected a subset of images of natural scenes, *i.e.* images without any human-made object, comprising of 274 images (first row in Fig. 2).

We then compute the distribution of pixel intensities, where each bin contains 16 intensity levels from an interval of [0;255] (Fig. 3). The histograms were obtained by using *i.* only the natural images and *ii.* all

images of the extended dataset. In this figure, each row depicts the results for the minimum operator in a small patch window using only the RED, GREEN and BLUE channels, the DCP (dark channel in all channels) and the UDCP (dark channel in green and blue).

Fig. 2 - Sample images of our dataset. The first row shows the images of natural scenes and the second row shows scenes that include human-made structures/objects (Images acquired from SUN Dataset [10]).

Even thou our datasets and those of He and colleagues are different, ours were collected using the same guidelines as theirs, and thus, some similarity is to be expected. Indeed, the histograms present similarities, but also important differences. The probability of the first bin (intensities between 0-15) is smaller than the one presented by He and colleagues [1]. They reported ≈ 90% for the first bin in the DCP while the probability for our dataset is ≈ 45% (Fig. 3). One can see the highest probability, ≈ 50%, is obtained for histograms of natural scenes (Fig. 3 - 1st and 3rd rows) which is the expected case of typical underwater scenes. The most important observation is related to the significance of each channel for the prior. The lower intensity bins of the blue channel (Fig. 3) are dominant mainly in natural scenes. The red channel is still dark but it is the most equalized histogram for all scenarios. The green channel presents similar behavior. Thus, the absence of blue color in the final composition of the scene represents the prevalence of this channel in both the DCP and the UDCP.

One can observe the close similarities between DCP and UDCP statistics in the histogram in Fig. 3. We show the Pearson's linear correlation coefficient in Table I, which quantifies these similarities. The correlation coefficient ranges from [-1;1], where a coefficient value close to one indicates that the relationship is almost perfect and negative values show that data are uncorrelated.

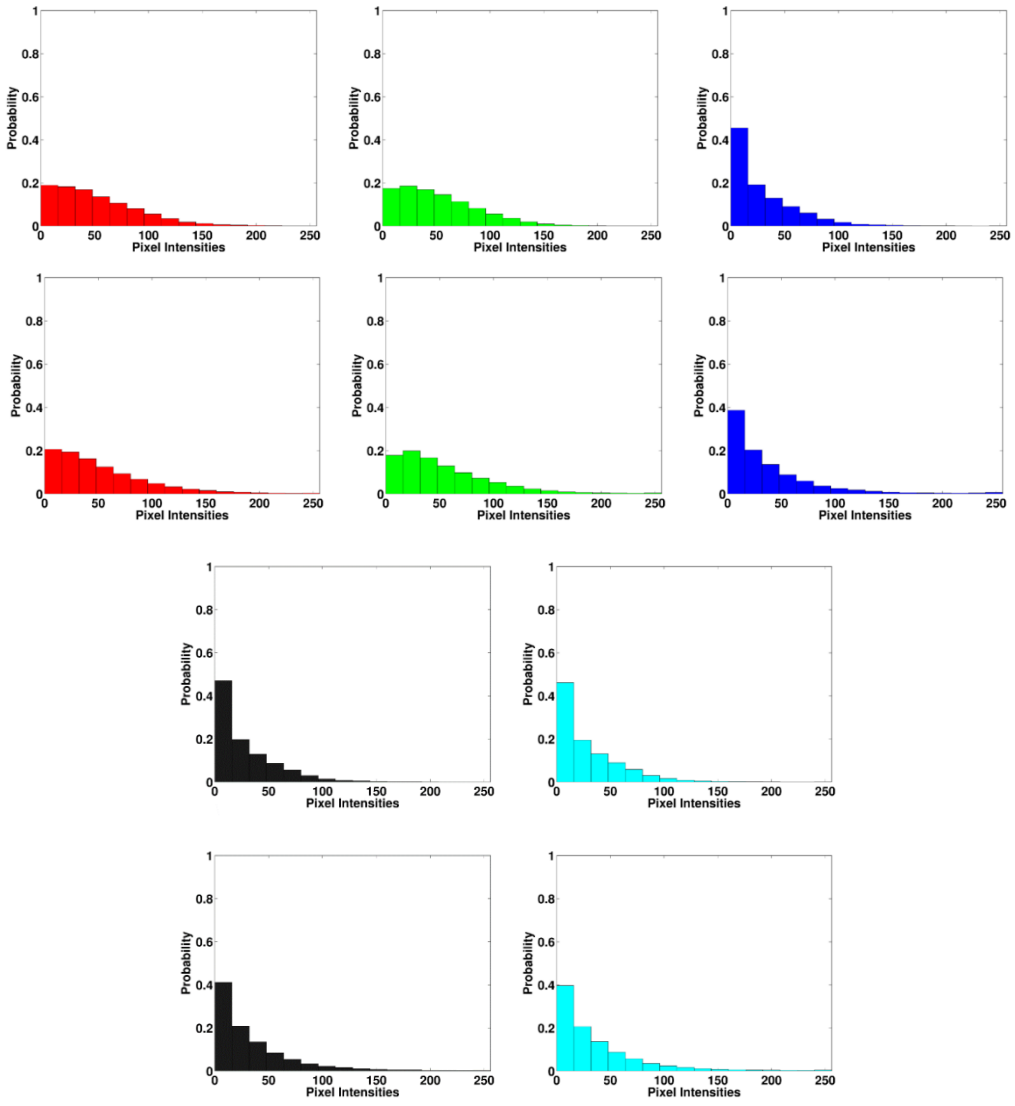

Fig. 3 - The distribution of pixel intensity of the dark channel for natural scenes of the extended dataset (1st and 3rd rows) and for all images of the extended dataset (2nd and 4th rows). We show the histogram for the red, green, blue channels, DCP (in black color), and UDCP (in cyan color), respectively.

Table I – Person's Correlation coefficient between DCP and UDCP, Red, Green and Blue channels.

	Natural Scenes	Extended Dataset
UDCP	0.9999	0.9998
Red	0.8049	0.8856
Green	0.7680	0.8351
Blue	0.9998	0.9995

One can readily see that there is a strong correlation between DCP and UDCP, which means that both methods are based on similar assumptions about the scene*, i.e.* low intensity dark channel. The value of the correlation coefficients for the blue channel and DCP are approximately equal to one meaning that they are also strongly correlated. In natural scenes, the correlation between DCP and green channel is the smallest due to the presence of grass and trees in the scenes, which causes an increase in the intensities of this color channel.

Fig. 4 – Sample images from the underwater datasets. Images from the *reduced* dataset are shown in the top row and images from the *extended* dataset is shown in the bottom row (First Row – Courtesy of Rémi Forget, Second Row—Courtesy of Kristina Maze).

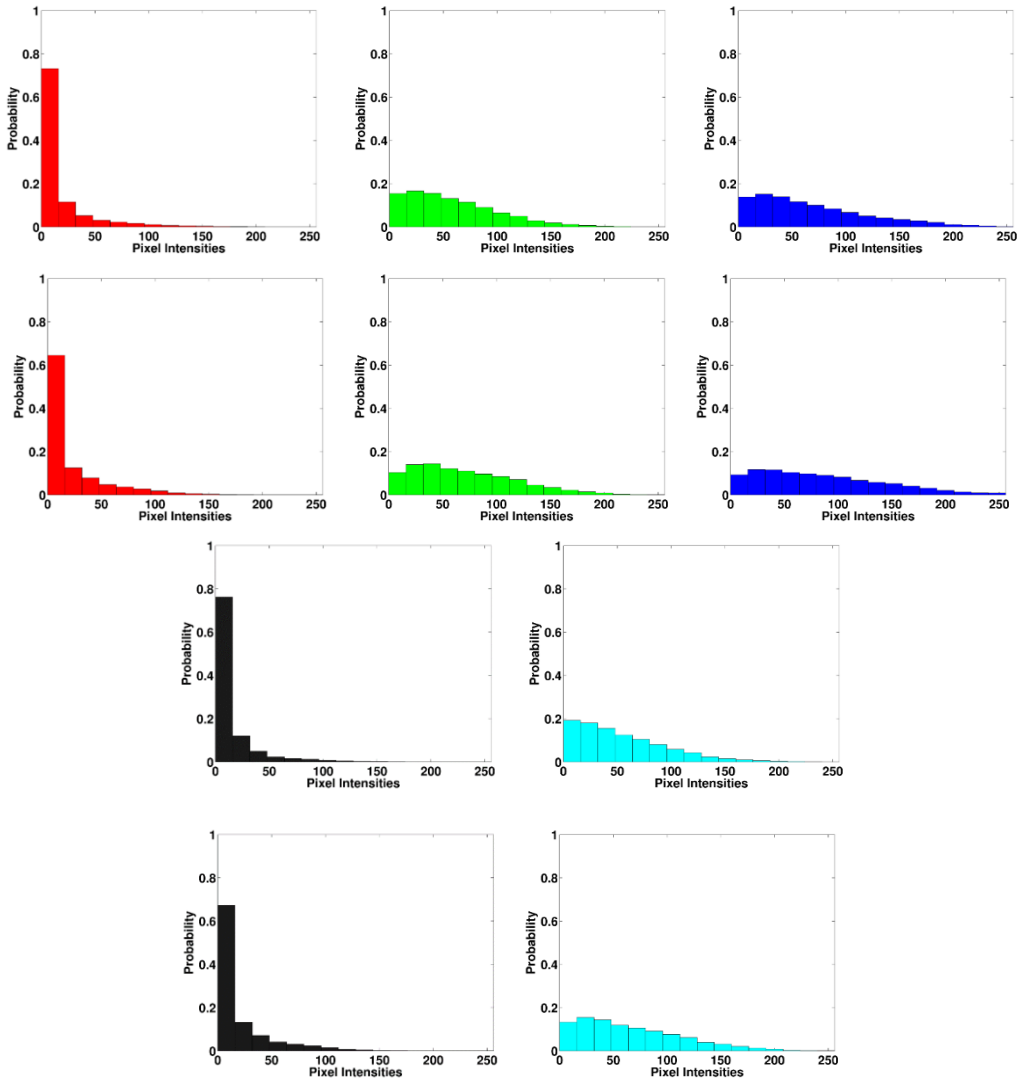

Fig. 5 - The distribution of pixel intensity of the dark channel for the reduced dataset (1st and 3rd rows) and for the extended dataset (2nd and 4th rows). We show the histogram for the red, green, blue channels, DCP (in black color), and UDCP (in cyan color), respectively.

We also created two datasets of underwater images to evaluate the influence of the medium and to verify the UDCP assumptions. The datasets creation follows the guidelines of He and colleagues [1]. The first dataset (**reduced**) was created by extracting the images from a single user of the Flickr website. This dataset contains 65 high quality photos acquired with the same camera. The images, which include coral reefs, rocks, marine animals, wreck, etc., were acquired during diving activities in several places of the

world (thus with different turbidity levels). The first row of Fig. 4 shows sample images of the reduced dataset.

The second dataset (**extended**) was obtained by collecting images from several image search engines on the internet. This dataset is composed of 171 underwater images acquired under diverse media conditions, water depth and scenes, which provides a rich source of information. All the images are approximately homogeneous illuminated that limits the water depth to shallow water. The second row of the Fig. 4 shows sample images of the extended dataset.

Differently from the histograms of outdoor scenes, the dark channel of the red channel is really dark, *i.e.* ≈ 90% of the pixels are in the first bin (Fig. 5). This agrees with the assumption of UDCP, *i.e.* the highest absorption rate for the red channel. As expected, the dark channel for the blue and the green channels are similar but many values cover a broader range due to the effects of the interaction of light with the medium. The histograms of DCP are somewhat consistent with what we would expect for non-participating media. Hence, DCP is not able to recover adequately the medium transmission. However, the bin values in the UDCP histograms are more evenly distributed, which indicates that UDCP is a better approach to estimate the medium transmission.

Experimental verification shows that the statistics for the UDCP assumption is a more general supposition than the DCP assumption. However, these results do not guarantee the quality of the estimated transmission. UDCP and DCP obtain similar histograms for natural scenes, as shown by the correlation analysis. These results indicate that both are based on similar assumptions.

Another important characteristic concerns the blue channel, which in natural scenes tends to be darker than the other channels. The underwater medium is typically blue, thus increasing the intensities of this color channel. This fact corroborates the underwater dark channel assumption.

Experimental Results

If from the one hand the experiments showed that the assumptions of UDCP are valid, on the other hand it is important to find out if the UDCP outperforms the other DCP based methods for restoring images. In order to evaluate the performance of UDCP, we applied the standard DCP to underwater images, as proposed by Chao and Wang [5], and Chiang and Chen [6]. The MDCP [8] was also applied to underwater images, but with the refinement proposed by He and colleagues [1]. We also obtained results for Bianco's prior (BP) [9]. Our evaluation is based on qualitative and quantitative analysis. Figs. 6 and 7 show the qualitative results for underwater images collected from the internet. Fig. 8 shows the sample of images from three underwater videos that we captured. We acquired these videos in a coral reef at the Brazilian Northeast Coastal area at the depth of approximately 10m. They are composed of 150, 138 and 610 frames, and the sample images of these videos are figs. 8(a), 8(b) and 8(c), respectively.

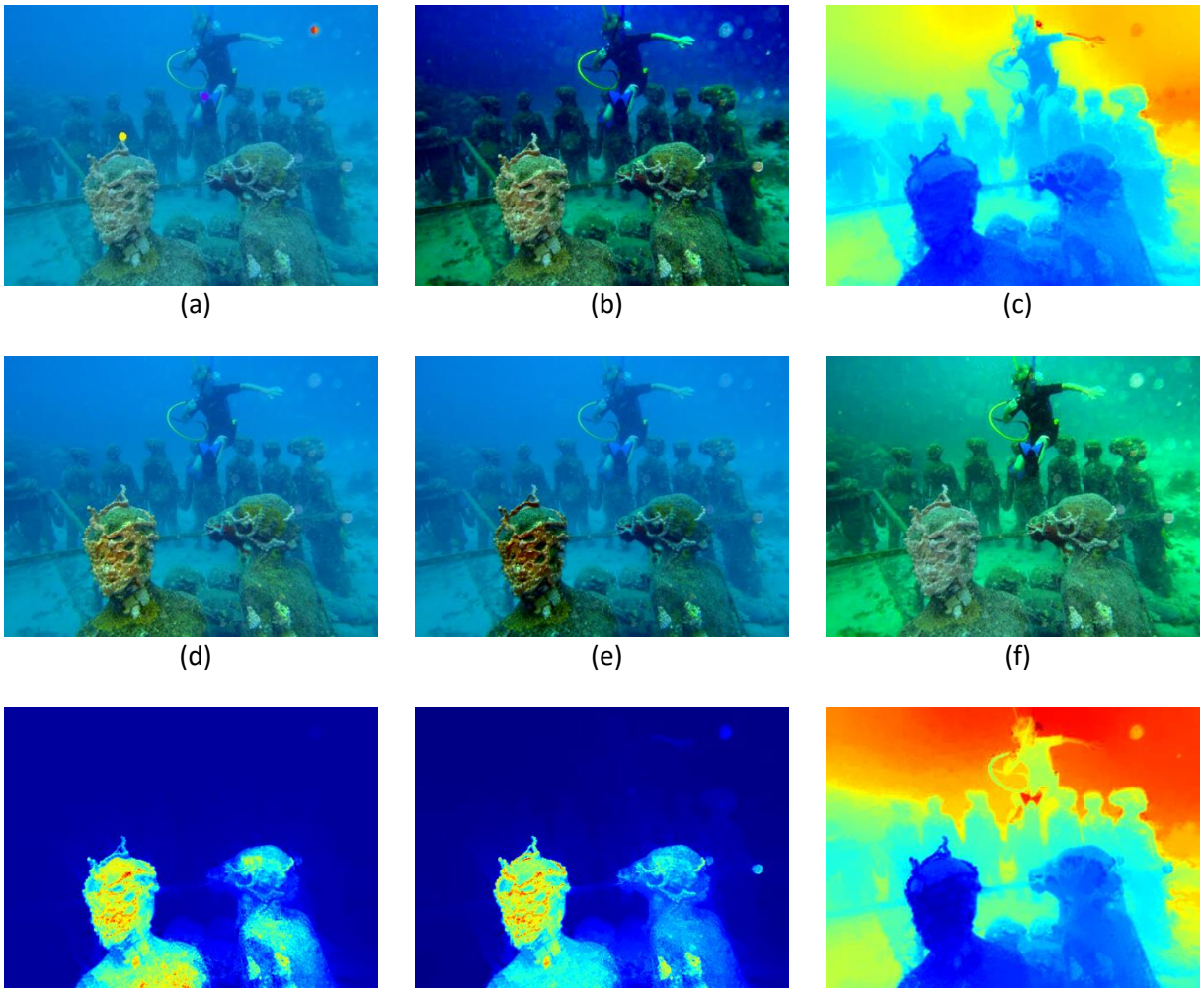

Fig. 6 – Restored images and depth estimation: (a) Underwater image with regions where the backscattering constant was estimated, using UDCP (orange patch), DCP (red patch), MDCP (yellow patch), and the BP (purple patch). Restored images using UDCP (b), DCP (d), MDCP (e), and BP (f). Colorized depth maps obtained using UDCP (c), DCP (g), MDCP (h), and BP (i) (The credits of the image (a): Kevin Clarke).

In the quantitative evaluation, we used a metric called τ proposed by Nicolas Hautière and colleagues [11] to analyze their method for weather-degraded images. We adopted this metric in the present work due to the similarities of weather-degraded image and underwater images. Three different indexes are defined in the τ metric: *e*, $\bar{r}$ and *s*. The value of *e* evaluates the ability of a method to restore edges, which were not visible in the degraded image, but are visible in the restored image. The value of $\bar{r}$ measures the quality of the contrast restoration; a similar technique was adopted by [3] to evaluate restoration in One example of these experiments is depicted in Fig. 6, which shows the original image, Fig. 6(a), the

restored image, Fig. 6(b), and the colorized depth maps, Fig. 6(c), obtained using UDCP approach. We colorized the depth maps to aid the visualization, where reddish colors represent closer points and bluish colors, represent points that are further away.an underwater medium. Finally, the value of s is obtained from the amount of pixels which are saturated (black or white) after applying the restoration method but were not before. These three indexes allow us to estimate an empirical restoration score $\tau = e + \bar{r} + 1 - s$ [11], where larger values mean better restoration. Table II shows the obtained results.

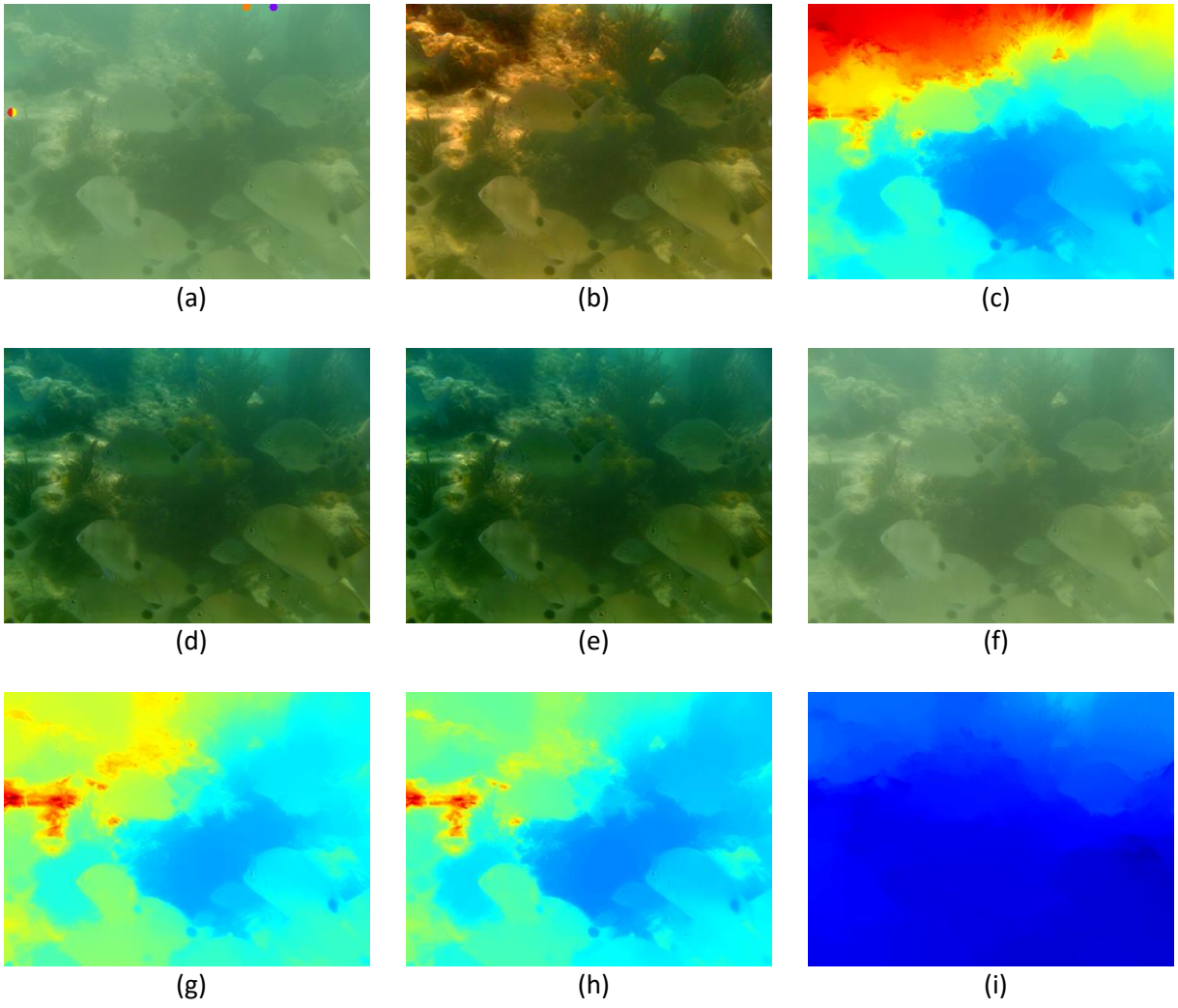

Fig. 7 – A second example of restored images and depth estimation: (a) Underwater image with regions where the backscattering constant was estimated, using UDCP (orange patch), DCP (red patch), MDCP (yellow patch), and the BP (purple patch). Restored images using UDCP (b), DCP (d), MDCP (e), and BP (f). Colorized depth maps obtained using UDCP (c), DCP (g), MDCP (h), and BP (i). (The credits of the image (a): Ancuti and colleagues [12]).

One example of these experiments is depicted in Fig. 6, which shows the original image, Fig. 6(a), the restored image, Fig. 6(b), and the colorized depth maps, Fig. 6(c), obtained using UDCP approach. We colorized the depth maps to aid the visualization, where reddish colors represent closer points and bluish colors, represent points that are further away.

Figs. 6 and 7 also show the results obtained by applying the methods proposed by other authors, (*i.e.* DCP, MDCP, and BP) on images from the extended dataset. This dataset is detailed in Section Underwater Dark Channel Prior and the Image Restoration. We show the underwater images with the back scattering light estimation in figs. 6(a) and 7(a). The estimation of the backscattering constant obtained by UDCP seems to be the most plausible, *i.e.* near the farthest point in the image. The other methods fail in the estimation in at least one of the images. They identify the backscattering light in bright surfaces of the scene instead of the farthest point.

Table II – Quantitative evaluation of the underwater restoration methods using the τ metric [11]. The best method is highlighted using bold letters. We show the results for the sample images in Figs. 6, 7 and 8 and the average of the extended dataset and the videos of Fig. 8.

	UDCP	DCP	MDCP	BP
Fig. 6(a)	**4.52**	2.22	2.14	3.50
Fig. 7(a)	**60.43**	41.44	56.97	3.01
Average of the Extended Dataset	**3.68**	2.77	2.75	3.01
Fig. 8(a)	**705.61**	640.95	641.72	2.85
Average of the Video 1	**3460.2**	1500.0	1942.8	2.79
Fig. 8(b)	**5.82**	5.49	4.80	2.21
Average of the Video 2	**32.02**	23.09	24.09	2.30
Fig. 8(c)	**10.81**	9.56	8.98	2.23
Average of the Video 3	**90.37**	69.56	73.11	2.36

The restored images by UDCP, figs. 6(b) and 7(b), show that there was an improvement as far as contrast and color fidelity are concerned. The values in Table II show that the restoration using UDCP presented the best values for τ metric for all experiments, including full dataset. In Fig. 6, the UDCP (b) and BP (f) presented the best results for contrast and visibility. However, BP fails to estimate the backscattering constant. It generates an incorrect depth information shown by the colorization of the restored image. This is corroborated by the fact that the depth maps estimated by both methods are similar. The improvement in the estimation of the ocean floor of the scene is noticed for the image restored using UDCP. The improvement provided by DCP and MDCP is imperceptible because both methods are not able to recover the depth map in a correct way.

The UDCP method obtained the best results in Fig. 7, while the BP, Fig. 7(f), presented the worst results. The values in Table II also confirm this fact. This can be explained since BP underestimates the attenuation

coefficient, limiting the quality of the map. This is due to the behavior of the red channel, which is not completely absorbed. The results obtained by standard DCP, Fig. 7(d), and MDCP, Fig. 7(e), are also related to this fact, since both methods are able to provide good results for depth map and restoration.

Fig. 8 shows the results obtained by applying the methods to the videos that we have captured. We depicted one sample image from each video, shown in figs. 8(a), 8(b) and 8(c). For these sample images, the backscattering constant is well balanced in all wavelengths due to the characteristics of the water and the small water depth. In this case, the standard DCP, MDCP and UDCP present similar results in qualitative terms. The BP method fails to estimate the depth map, in a similar way as the one shown in Fig. 7. Thus, we omit the results using BP because they are similar to those obtained by the underwater camera, *i.e.* first row. The UDCP attained the best results for scenes located at greater depths, evidenced by the visibility of the rock in the top left of the restored image in Fig. 8(i).

Table II shows the average values for the videos illustrated by sample images in Fig. 8. We can clearly see that our method presents better results using the τ metric, especially due to its ability to improve edges. The average of the extended dataset is also shown, and the results are still favorable to UDCP. One can see that the τ metric presents large values for video associated to Fig. 8(a). This is because the number of edges in the underwater image is small, assuming the parameters adopted by Hautière and colleagues [11]. The increase provided by the restoration is large, producing large values of the *e* metric and, by consequence, the τ metric.

Conclusions

Although the standard DCP is intuitive, it has shown limitations to its use in underwater conditions because of the high absorption of the red channel. The BP method presented good results in specific contexts, but it underestimated medium transmission. The MDCP presents similar results to the DCP. Finally, UDCP presented the most significant results in underwater conditions. It provides good restoration and depth estimation even in situations where other methods can fail.

Despite the fact that UDCP presented meaningful results, it lacks both in reliability and robustness due to the limitations imposed by the assumptions. On the one hand, the use of single image methods to restore images can enhance the quality, but on the other hand, it is susceptible to the variations in scene characteristics. Thus, one important direction is to use the information provided by the image to estimate a confidence level, which would prove to be useful in practical applications, *e.g.* robotics. Another important direction to be pursued is to use image sequences to disambiguate the parameters of the model. Video acquisition is a common capability in almost all types of underwater cameras commonly used by divers and ROVs. In this case, a single image restoration method can be used for initial estimation, which would be followed by successive refinements as other images become available. Finally, for several applications, it might be necessary to enhance the model with the inclusion of the effect of artificial illumination in the scene. It will enable us to deal with deep-water conditions.

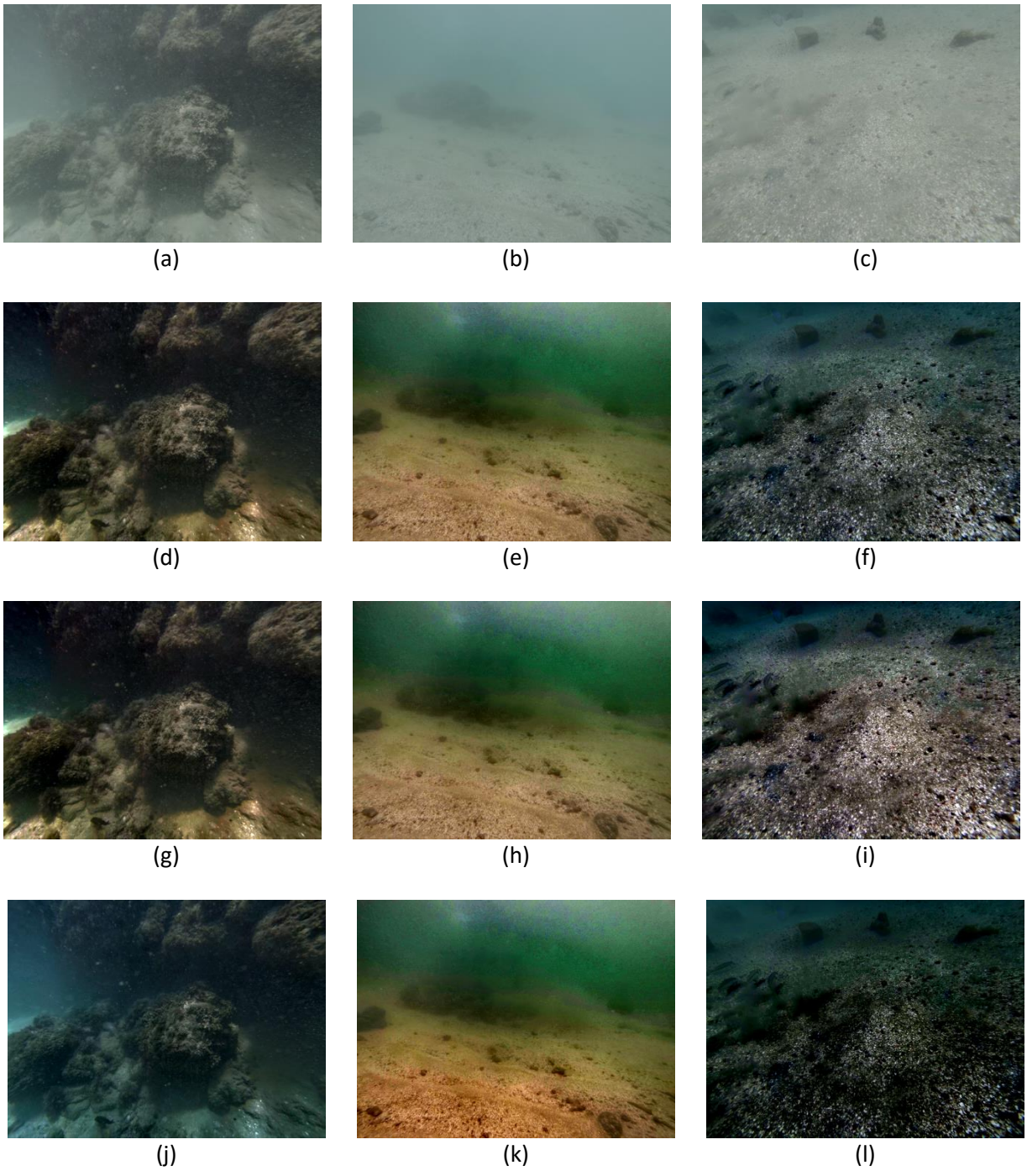

Fig. 8 – Image restoration of three underwater videos acquired in Brazilian Northeast Coastal area. The first row shows three sample images for each video. The restoration results for these sample images obtained by the standard DCP, UDCP and MDCP are shown in the second, third and fourth rows, respectively.

References

[1] K. He, J. Sun, and X. Tang. Single image haze removal using dark channel prior, in IEEE CVPR, pages 1956–1963, 2009.
[2] P. Drews-Jr, E. Nascimento, F. Moraes, S. Botelho, M. Campos, Transmission estimation in underwater single images, in IEEE ICCV - Workshop on Underwater Vision, 2013, pp. 825–830.

[3] Y. Schechner and N. Karpel. Recovery of underwater visibility and structure by polarization analysis. IEEE JOE, 30(3):570–587, 2005.

[4] R. Fattal. Single image dehazing. ACM TOG, 27(3), 2008.

[5] L. Chao and M. Wang. Removal of water scattering, in ICCET, volume 2, pages 35–39, 2010.

[6] J. Chiang and Y. Chen. Underwater image enhancement by wavelength compensation and dehazing. IEEE TIP, 21(4):1756–1769, 2012.

[7] S. Serikawa and H. Lu. Underwater image dehazing using joint trilateral filter. Computers & Electrical Engineering, 40(1): 41–50, 2014.

[8] K. Gibson, D. Vo, and T. Nguyen. An investigation of dehazing effects on image and video coding. IEEE TIP, 21(2):662–673, 2012.

[9] N. Carlevaris-Bianco, A. Mohan, and R. Eustice. Initial results in underwater single image dehazing, in IEEE OCEANS, pages 1–8, 2010.

[10] J. Xiao, J. Hays, K. Ehinger, A. Oliva, A. Torralba. SUN database: Large-scale scene recognition from abbey to zoo, in IEEE CVPR, pp. 3485–3492, 2010.

[11] N. Hautière, J.-P. Tarel, D. Aubert and E. Dumont. Blind contrast enhancement assessment by gradient ratioing at visible edges. Image Analysis & Stereology, 27(2): 87–95, 2008.

[12] C. Ancuti, C. Ancuti, T. Haber, and P. Bekaert. Enhancing underwater images and videos by fusion. In IEEE CVPR, pages 81-88, 2012.